Ionization energies of ClO and Cl2O2

ARTICLE *in* THE JOURNAL OF PHYSICAL CHEMISTRY · JUNE 1996

Impact Factor: 2.78 · DOI: 10.1021/jp9602585

6 AUTHORS, INCLUDING:

Martin Schwell

Université Paris-Est Créteil Val de Marne - UPEC

62 PUBLICATIONS **754** CITATIONS

SEE PROFILE

Ionization Energies of ClO and Cl_2O_2

M. Schwell,[†] H.-W. Jochims,[†] B. Wassermann,[†,‡] U. Rockland,[†] R. Flesch,[†,‡] and E. Rühl*,[†,‡]

Institut für Physikalische und Theoretische Chemie, Freie Universität Berlin, Takustr. 3, D-14195 Berlin, Germany, and Institut für Physik, Johannes Gutenberg-Universität Mainz, D-55099 Mainz, Germany

Received: January 25, 1996; In Final Form: April 4, 1996[⊗]

The ionization energies of chlorine oxide (ClO) and its dimer (Cl_2O_2) have been measured using monochromatic synchrotron radiation in the 10−20 eV energy regime in combination with photoionization mass spectrometry. The threshold energy of ClO^+ ($m/z = 51$) is found at 10.85 ± 0.05 eV, whereas the ionization threshold of $Cl_2O_2^+$ ($m/z = 102$) occurs at 11.05 ± 0.05 eV. The experimental values are compared to results from *ab initio* calculations, where three stable isomers of Cl_2O_2 are considered: dichlorine peroxide (ClOOCl), chloryl chloride ($ClClO_2$), and chlorine chlorite (ClOClO). The results indicate that the experimental threshold energy of $Cl_2O_2^+$ is due to adiabatic ionization of ClOOCl. The heat of formation of $ClOOCl^+$ is derived from the ionization threshold: $\Delta_f H^0_{298}(ClOOCl^+) = 1203 \pm 12$ kJ/mol. Evidence for the occurrence of less stable Cl_2O_2 isomers, such as $ClClO_2$ and ClOClO, is obtained from appearance energy measurements of the $OClO^+$ ($m/z = 67$) fragment cation. The shift in ionization energy of ClOOCl relative to ClO is compared to other dimers of radicals, such as HO and NO_2.

Introduction

Chlorine oxide ClO is of general interest because of its considerable mixing ratio in the stratosphere.[1] It has been found that the ClO mixing ratio is strongly anti correlated to that of ozone in the austral spring. Consequently, it is generally assumed that the ClO radical plays a key role in polar ozone depletion.[1,2] ClO is formed in the reaction of chlorine atoms with ozone. The major source of chlorine atoms is now believed to come from the photolysis of chlorofluoro hydrocarbons (CFCs) which are finally converted into active chlorine species, such as Cl_2 or HOCl. These compounds are formed via heterogeneous reaction during the polar night.[3] Efficient photolysis of Cl_2 and HOCl right after sunrise induces efficient formation of chlorine atoms which in turn, induce massive ozone loss in the stratosphere. The mechanisms of polar stratospheric cloud (PSC) formation leading to heterogeneous chlorine activation are still controversial.[4]

More recent results suggested that a stable dimer of ClO can be formed at low temperatures.[5] This is especially true for Antarctica, where the average temperature is lower than in the Arctic. The role of Cl_2O_2 in the stratosphere is therefore crucially connected to its rate of formation, its photochemical decay routes, and the formation of different isomers in the three-body self-reaction of ClO. Catalytic cycles involving the ClO dimer have been postulated, including their possible importance with respect to polar ozone depletion, showing that the ClO dimer is one of the key compounds needed to understand the fast decay of the ozone concentration right after the end of the polar night.[5a]

Since the discovery of the importance of the ClO dimer various experimental and theoretical studies have been performed in order to obtain more information on the properties of this species. These include studies on the structure of Cl_2O_2 isomers,[6,7] their thermodynamic stability,[7] the infrared[8] and UV absorption cross section,[9−12] as well as photolysis reactions.[8,11,13]

However, there are still quite a few properties of ClO and Cl_2O_2 that remain unknown, which include ionization energies. To date, neither species has been isolated and/or purified. They have mostly been obtained in flow tube systems and in gas cells along with various other compounds.[9−12] Photoionization of ClO has been studied earlier by photoelectron spectroscopy.[14,15] These results indicate that the photoelectron spectrum of ClO is strongly contaminated by the reactants which form ClO.

We have applied photoionization mass spectrometry in order to measure the ionization energy (IE) of ClO and the ClO dimer (Cl_2O_2). Mass spectrometry allows one to selectively detect ions at a specific mass channel, thus efficiently discriminating against other reactants and products occurring in the flow tube synthesis. Earlier experiments using electron impact ionization[16] showed that the parent cation $Cl_2O_2^+$ ($m/z = 102, 104, 106$) is stable. Therefore, a combination of mass spectrometry with a tunable vacuum ultraviolet light source, such as synchrotron radiation, is well suited to measure the ionization energy of Cl_2O_2.

Experimental Section

Chlorine oxide is produced by the reaction of atomic chlorine with ozone in a flow tube. The flow tube consists of a 600 mm long and 20 mm diameter glass tube that is coated with halocarbon wax. The tube is evacuated by a rotary pump (Edwards, pump speed: 20 m^3/h). A 10% Cl_2/He mixture passes through a microwave discharge, where atomic chlorine is formed. The ozone is produced by flowing neat oxygen through a commercial laboratory ozonizer (Sander). The O_3/O_2 mixture containing about 3% ozone is introduced into the flow tube without further purification where it reacts with the chlorine atoms. The flow speed is estimated to be approximately 2−5 m/s at a typical total pressure of 5−7 mbar in the reactor, which is measured by a capacitance manometer (Baratron). The partial pressures of both reactants are optimized by maximizing the ClO^+ yield ($m/z = 51, 53$) using photoionization mass spectrometry. Dimers of ClO are also formed in the flow tube if it is cooled to 198 K by a surrounding jacket containing methanol from a cryostat (Lauda). Typically, we find that the $Cl_2O_2^+$ signal ($m/z = 102, 104, 106$) intensity is up to 10% of the ClO^+ signal ($m/z = 51, 53$) using photoionization mass spectrometry at 15 eV photon energy. This fraction

[†] Freie Universität Berlin.
[‡] Johannes Gutenberg-Universität Mainz.
[⊗] Abstract published in *Advance ACS Abstracts,* May 15, 1996.

S0022-3654(96)00258-4 CCC: $12.00

may be different from the neutral ClO/Cl_2O_2 mixing ratio in the flow tube because of ionic fragmentation and different ionization cross sections of both species. Efficient production of the Cl_2O_2 occurred only when there was an excess of ozone relative to chlorine in the flow system. This is consistent with the fact that the competing reaction $Cl + Cl_2O_2 \rightarrow Cl_2 + ClOO$ efficiently destroys the ClO dimer.[9]

A portion of the flowing gas mixture leaks through a 1 mm diameter hole into an expansion chamber which is equipped with a diffusion pump (Norton, pump speed: 2450 L/s). The gas beam passes through a 500 μm skimmer into the ionization region of a time-of-flight mass spectrometer which is operated according to the Wiley/McLaren space focusing conditions.[17] Further experimental details of the TOF-MS have been published earlier.[18] We have chosen the TOF-MS instead of a quadrupole mass spectrometer, which was used in previous work,[19] because of its capability to measure *simultaneously* up to three photoion yield spectra of mass selected cations. The use of a time-of-flight mass spectrometer is especially desirable in our flow tube experiment in order to control instabilities in the flow system. Mass selection is accomplished by using gated amplifiers (Tennelec 454), triggered by the high voltage pulse which extracts the cations from the ionization region (pulse width: 1−2 μs, field strength: 300 V/cm) and gate and delay generators (LeCroy 222). The typical pressure in the ionization region is on the order of 10^{-5} mbar in order to avoid secondary collision processes. The sample is ionized by monochromatic synchrotron radiation provided by the Berlin electron storage ring BESSY using a modified 1.5 m normal incidence monochromator (McPherson 225; grating: 1200 L/mm coated with Al/MgF_2; wavelength resolution 0.2 nm). Energy calibration is obtained by recording the well-known photoion yield spectrum of molecular oxygen.[20] The spectra are normalized to the VUV photon flux (i.e., storage ring current and transmission function of the grating). Ionization threshold measurements required the use of a LiF-cutoff-filter in order to avoid second-order light as well as high energy stray light.

Computational Details

Ab initio calculations are carried out using the GAMESS,[21] GAUSSIAN 94,[22] and MOLPRO[23] program packages on a CRAY Y-MP computer. Graphics output is generated on Silicon Graphics INDIGO workstations by using the UNICHEM program package (cf. ref 24).

Results and Discussion

Figure 1 shows a typical photoionization mass spectrum of the products leaving the flow tube under conditions where Cl_2O_2 is formed. The spectrum is recorded at 15 eV photon energy. The most intense mass peaks are due to O_2^+ (m/z = 32) and Cl_2^+ (m/z = 70, 72, 74). The products and their fragments ClO^+ (m/z = 51, 53), $Cl_2O_2^+$ (m/z = 102, 104, 106), and $OClO^+$ (m/z = 67, 69), traces of residual gas (H_2O^+ (m/z = 18), N_2^+ (m/z = 28)), as well as excess ozone (m/z = 48) occur with much weaker intensity. Chlorine-containing species are unambiguously identified by their natural isotope pattern.

Figure 2 shows the photoion yield curves of ClO^+ (m/z = 51) and $Cl_2O_2^+$ (m/z = 102) in the threshold regime between 10.5 and 11.5 eV recorded with an energy step width of 0.033 eV. Both curves were measured simultaneously using a lithium fluoride cutoff filter.

The threshold energy of ClO^+ formation is found at 10.85 ± 0.05 eV (Figure 2a). This value is in excellent agreement with the onset of the first photoelectron band of ClO reported by Bulgin et al.[14,15] The pulsed field of 300 V/cm which is applied

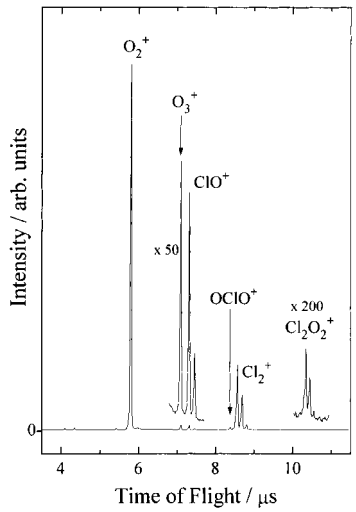

Figure 1. Time-of-flight mass spectrum of the $Cl + O_3$ reaction which is used for ClO and Cl_2O_2 production. Experimental conditions: 15 eV photon energy, $T_{flow\ tube}$ = 198 K, $p_{flow\ tube}$ = 7 mbar).

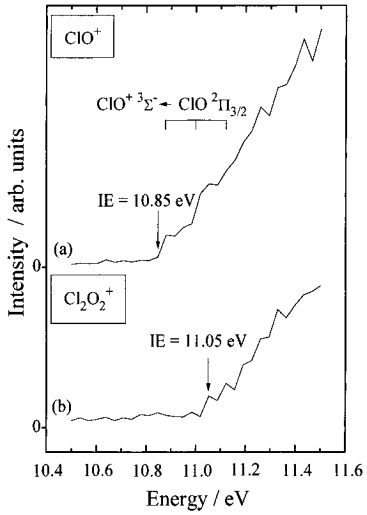

Figure 2. Photoion yield curves of (a) ClO^+ (m/z = 51) and (b) $Cl_2O_2^+$ (m/z = 102). The ionization energies (IE) are indicated by arrows. Both spectra are recorded with a LiF filter.

for accelerating the ions out of the ionization region is expected to shift the ionization energy by 13 meV to lower energy due to the Stark shift effect. This is well within the experimental error limit so that this minor effect is neglected in the following. The ClO^+ cation yield increases above threshold with characteristic steps at 10.87, 11.00, and 11.125 eV. This threshold behavior is typical for photoion yield curves of diatomic molecules.[25] Specifically, these steps are due to the Franck−Condon-dominated vibrational fine structure of the $ClO^+(X^3\Sigma^-)$ cation state corresponding to ClO^+ ($X^3\Sigma^-$, $v' = 0, 1, 2$) ← ClO ($X^2\Pi_{3/2}$) transitions (ω_e = 1040 ± 30 cm^{-1} [14]). Transitions from the $ClO(X^2\Pi_{1/2})$ state have been identified as weak shoulders in the photoelectron spectrum.[14] These close-lying features are evidently too weak to be observed in the photoion yield curve of ClO^+. Higher quality photoion yields, i.e., with higher signal strength, smaller energy step width, and higher energy resolution, would be required to resolve these features.

The threshold energy of $Cl_2O_2^+$ (m/z = 102) is observed at 11.05 ± 0.05 eV (Figure 2b). Additionally, we have measured mass spectra in the $Cl_2O_2^+$ threshold region in order to verify the threshold energy of the ClO dimer using acquisition times up to 300 s per mass spectrum. This is necessary to gain further sensitivity in threshold energy determination. These additional

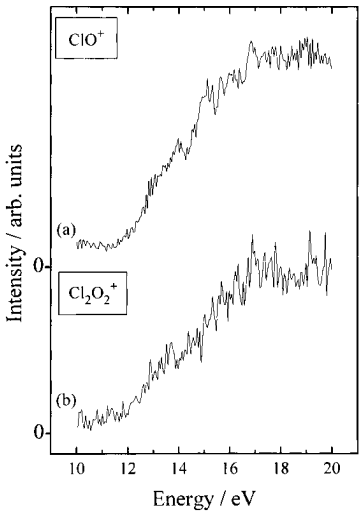

Figure 3. Photoion yield curves of (a) ClO^+ ($m/z = 51$) and (b) $Cl_2O_2^+$ ($m/z = 102$).

experiments lead to identical results as the photoion yield spectra shown in Figure 2.

The photoion yield curve of $Cl_2O_2^+$ shows no distinct vibrational fine structure in the threshold regime, contrary to the ClO^+ yield. The lack of vibrational structure may be the result of a higher density of vibrational states near the $Cl_2O_2^+$ threshold. Unfortunately, to our knowledge the photoelectron spectrum of Cl_2O_2 has not been reported. Thus, many properties of $Cl_2O_2^+$ including Franck−Condon factors are experimentally unknown. Other reasons for the lack of vibrational structure can be found in a superposition of superexcited neutral states which can also occur near the ionization threshold. Additionally, the orbital structure of the ClO dimer is expected to be more complex than that of ClO. Results from *ab initio* calculations, which will be discussed below in detail, indicate that another ionic state (second-highest occupied molecular orbital (SOMO)) is close to the highest occupied molecular orbital (HOMO) of Cl_2O_2 ($-\epsilon_{HOMO} = 12.707$ eV, $-\epsilon_{SOMO} = 12.880$ eV). Therefore, the threshold behavior of $Cl_2O_2^+$ may be connected to two different ionic states, which is equivalent to an increase in density of states in the threshold regime. Similar findings are reported for hydrogen peroxide (H_2O_2), where, in contrast to the OH radical, the first photoelectron band is broad and structureless as a result of two ionic states.[26,27]

Figure 3 shows photoion yield curves of ClO^+ ($m/z = 51$) and $Cl_2O_2^+$ ($m/z = 102$) in the 10−20 eV regime recorded with a step width of 0.05 eV. Both spectra are recorded without the LiF cutoff filter. They are normalized to the photon flux of the monochromator showing characteristic differences compared to the threshold regions displayed in Figure 2 which is a result of second-order light in the region below 12 eV. The statistics of both spectra is quite poor as a result of small signal strength. However, there are characteristic differences between both photoion yield curves: The ClO^+ cation yield curve (Figure 3a) consists of a continuous increase in intensity up to 17 eV. The curve is almost structureless; it shows several broad features which are superimposed to the continuous cation yield. Distinct maxima occur at 14.0, 15.0, and 16.8 eV, which are tentatively assigned to excitations of Rydberg states, autoionizing into the ClO^+ channel. It is known that photoion yield curves of molecules contain distinct resonances as a result of excitation of Rydberg states with low principal quantum number.[28] A plausible assignment can often be found by a comparison of the shape of such resonances to the corresponding photoelectron bands that are the convergence limits of Rydberg series.[28,29] In the case of ClO it is plausible that the resonance occurring at 14.0 eV is a result of the lowest member of a Rydberg series, which converges to the ionization energy of ClO at 16.3 eV ($7\sigma^{-1}$, $^3\Pi$[14,15]). This assignment is obtained by determining the quantum defect ($\delta = 0.57$) from the Rydberg formula, where the magnitude of δ is in the typical range for Rydberg states of p-symmetry. Other weak resonances are observed at higher excitation energies (15 and 16.8 eV), which are also likely due to Rydberg states with low principal quantum number. A firm assignment of these resonances cannot be given here.

TABLE 1: *Ab Initio* Calculations of the Vertical Ionization Energies (IE_v) of ClO and Three Isomers of Cl_2O_2[a]

molecule	$E_{neutral}$ (hartree)	E_{ion} (hartree)	zero point energy (eV)	IE_v (eV)
(a) MOLPRO MRCI/VTZ Basis Set				
ClO	−534.6946	−534.2719	0.053	11.45
ClOOCl	−1069.3596	−1068.925	0.1841	11.64
$ClClO_2$	−1069.3050	−1068.8940	0.2337	10.95
ClOClO	−1069.3075	−1068.9293	0.1767	10.11
(b) GAUSSIAN MP2/6-31G* Basis Set				
ClO	−534.5060	−534.0762	0.053	11.64
ClOOCl	−1069.0697	−1068.6355	0.1841	11.63
$ClClO_2$	−1069.0284	−1068.6351	0.2337	10.46
ClOClO	−1069.0361	−1068.6228	0.1767	11.07

basis set	SV-3-21G* IE_v (eV)	TZVP IE_v (eV)	SV-6-31G* IE_v (eV)
(c) GAMESS Green's Function Method, Second-Order Perturbation Theory			
ClOOCl	11.13	11.39	11.23
$ClClO_2$	10.38	10.9	10.7
ClOClO	10.12	10.85	10.63

[a] All geometries are optimized at the MP2/6-31 G* level.

In contrast, the photoion yield curve of $Cl_2O_2^+$ (Figure 3b) shows no distinct resonances. It is known that photoion yield curves of polyatomic molecules with low symmetry seldom contain pronounced resonances in the ionization continuum.[20] This is likely a result of the effective competition of neutral dissociation channels with autoionization.

There are three thermodynamically stable isomers of Cl_2O_2 according to recent *ab initio* calculations.[6,7,30−32] These are dichlorine peroxide (ClOOCl), chloryl chloride ($ClClO_2$), and chlorine chlorite (ClOClO). Another isomer, ClClOO, is of minor importance.[7] Recent theoretical work has already shown that dichlorine peroxide is the thermodynamically most stable isomer of Cl_2O_2, whereas $ClClO_2$ and ClOClO are by ∼4 and ∼42 kJ/mol less stable.[30] Therefore, the well-established UV absorption cross section of Cl_2O_2 that peaks at 243 nm is generally believed to be due to ClOOCl.[9,10,32]

We have carried out *ab initio* calculations in order to establish which of the various possible Cl_2O_2 isomers contributes to the experimental threshold energy of $Cl_2O_2^+$ ($m/z = 102$). The focus of our calculations are the first vertical ionization energies. The initial geometries are obtained from earlier work of McGrath et al.[6] The results are compiled in Table 1, where the use of different methods indicates that comparable results are obtained. This is particularly true for the relative order of the ionization energies of ClO, ClOOCl, $ClClO_2$, and ClOClO. The results indicate that the thermodynamically most stable isomer ClOOCl always gives the highest ionization energy compared to the other Cl_2O_2 isomers. Moreover, one observes a blue-shift of 0.19 eV of IE(ClOOCl) relative to IE(ClO) according to the MOLPRO MRCI/VTZ calculations, which is similar to the experimental blue-shift. On the other hand, results from GAUSSIAN MP2/6-31G* calculations indicate that IE(ClO) and IE(ClOOCl) are quite similar.

The best quantitative agreement with the experimental ionization energies is obtained by applying Green's function method, which is available in the GAMESS *ab initio* program package in conjunction with a 3-21G* basis set. The deepest 12 molecular orbitals are regarded as core orbitals which are not considered with respect to contributions to the ionization energy. The following 16 outer orbitals are considered to contribute to electron correlation effects on the ionization energy. Green's function method is only available for closed-shell species in the GAMESS program package. Therefore, the ionization energy of the radical ClO cannot be calculated in this frame. We have also calculated the vertical ionization energy of the chemically related Cl_2O molecule in order to verify the accuracy of this method. We also find in this case a remarkable quantitative agreement between both values ($IE\text{-}(Cl_2O)_v^{exp} = 11.02$ eV;[33] $IE(Cl_2O)_v^{calc} = 11.07$ eV).

The vertical ionization energy of ClOOCl is 11.13 eV according to Green's function method (see Table 1c). The calculations indicate that the vertical ionization energies of the other isomers are considerably lower in energy (see Table 1c). Larger basis sets have been also used giving similar results (cf. Table 1c), which are somewhat higher than the vertical ionization energies obtained from the 3-21G* basis set.

Additional calculations were performed in order to obtain further information whether the adiabatic ionization energy of ClOOCl differs from its vertical ionization energy. The cation energy is obtained using a 6-311G* basis set, where the ClO−OCl bond is shortened by 0.07 Å and a planar trans-geometry is reached. The results indicate that the adiabatic ionization energy of ClOOCl is 0.15 eV below the vertical values, which are listed in Table 1. It is concluded that the experimental threshold energy of $ClOOCl^+$ formation is close to the adiabatic ionization energy.

We believe as another result of the calculations that the experimental ionization threshold of $Cl_2O_2^+$ ($m/z = 102$) reflects the formation of ClOOCl via the termolecular self-reaction of ClO in the flow system. This result is in agreement with earlier experiments in which ClOOCl has been detected to be the dominant dimerization product. We can also conclude that other Cl_2O_2 isomers, if present, do not form stable parent cations when they are ionized (see below); thus, the mass signal at $m/z = 102$ exclusively reflects ionization of ClOOCl.

It is noted that there is also experimental evidence that the other isomers $ClClO_2$ and ClOClO are possibly formed in the flow tube system, which are likely to decompose into $OClO^+$ via ionic fragmentation. This is evidenced by determining the appearance energy of $OClO^+$ ($m/z = 67, 69$) at 10.95 ± 0.1 eV from a series of mass spectra, which are presented in Figure 4. This value is considerably higher than the ionization energy of neutral OClO ($IE(OClO) = 10.33 \pm 0.02$ eV[34]), indicating that $OClO^+$ is not efficiently formed as a neutral species in the cold flow system. Schindler and co-workers have noted earlier that $OClO^+$ is observed in electron impact mass spectrometry which is used to monitor Cl_2O_2 formation, if the flow system is coated with ice−water.[35] It is thought that possibly heterogeneous reactions of ClO involving the ice-coated wall of the flow tube lead to the formation of $ClClO_2$.[35] The mechanism of $ClClO_2$ formation under these conditions is not clear yet, but it has been verified by electron impact mass spectrometry of $ClClO_2$ that the parent cation ($m/z = 102, 104, 106$) is not stable and $OClO^+$ occurs as a fragment.[36] This finding suggests that $ClClO_2$ may also be the source of the $OClO^+$ signal in our photoionization experiment. On the other hand, ionization and subsequent fragmentation of the less stable isomer ClOClO will also yield $OClO^+$ by the loss of a neutral chlorine atom. Therefore, it cannot be decided at this stage which of the two isomers contributes to the $OClO^+$ signal. We will next discuss this question with respect to thermochemical considerations.

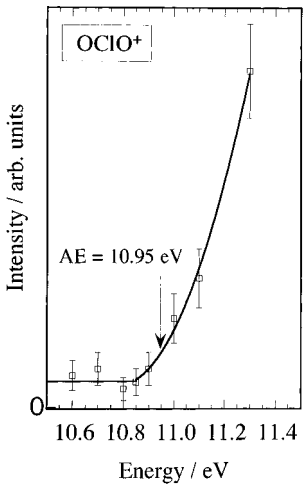

Figure 4. Photoion yield curve of $OClO^+$ ($m/z = 67, 69$). The data points (open squares) are obtained by integrating the $OClO^+$-mass regime in time-of-flight mass spectra. Solid lines are inserted to guide the eye. The appearance energy (AE), which is indicated by an arrow, corresponds to the energy where the $OClO^+$ signal exceeds the background level.

Thermochemical data of cations and their fragments have been successfully derived from ionization energies and fragment appearance potentials.[25,37] We use the stationary electron convention and assume that charged species have the same heat capacities as the corresponding neutrals.

The ionization energy of ClOOCl ($IE(Cl_2O_2) = 11.05 \pm 0.05$ eV) is used to derive the heat of formation of $ClOOCl^+$, which has not been reported earlier to our knowledge. The heat of formation of the neutral dimer is 133 ± 8 kJ/mol (at $T = 298$ K) according to ref 38. This gives $\Delta_f H^0_{298}(ClOOCl^+) = 1203 \pm 12$ kJ/mol considering that the experiments were performed at $T = 198$ K.

The dimer ionization energy may, in turn, be used to derive the bond dissociation energy in the ionic dimer. Using the thermochemical reference data quoted in ref 38, one obtains $D_{298}(ClO{-}OCl^+) = 48 \pm 18$ kJ/mol. This value is somewhat lower than the bond dissociation energy of the neutral dimer ($D_{298}(ClO{-}OCl) = 70 \pm 8$ kJ/mol[38]), which is an indication that ionization slightly weakens the O−O bond in the dimer, and a stable dimer cation is observable in mass spectra. This will be discussed in the following text in conjunction with the results from *ab initio* calculations.

The appearance energy of $OClO^+$ ($AE(OClO^+) = 10.95 \pm 0.1$ eV) is used to derive the heat of formation of the neutral dimer isomer according to: $Cl_2O_2 + h\nu \rightarrow OClO^+ + Cl + e^-$. With $\Delta_f H^0_{298}(OClO^+) = 1096 \pm 5$ kJ/mol[39,40] and $\Delta_f H^0_{298}(Cl) = 121.679$ kJ/mol[41] and thermal corrections[37] one obtains $\Delta_f H^0_{298}(Cl_2O_2) = 160 \pm 14$ kJ/mol, assuming that the ionic fragmentation threshold contains no excess energy and the products are formed in their ground states. This value appears to be quite reasonable if it is compared to $\Delta_f H^0_{298}(ClOOCl) = 133 \pm 8$ kJ/mol:[38] The difference in heat of formation of both isomers is therefore 27 ± 22 kJ/mol, which is in the energy range that has been considered for both less stable isomers of Cl_2O_2.[30] Results from the highest level *ab initio* calculations indicate that $ClClO_2$ is 4 kJ/mol[6,30] and ClOClO is 29 kJ/mol[6] or 42 kJ/mol[30] less stable than ClOOCl. A comparison with the above-calculated difference in heat of formation (27 ± 22 kJ/mol) indicates that $OClO^+$ formation is most likely the result of $ClOClO^+$ fragmentation. However, ionic fragmentation of

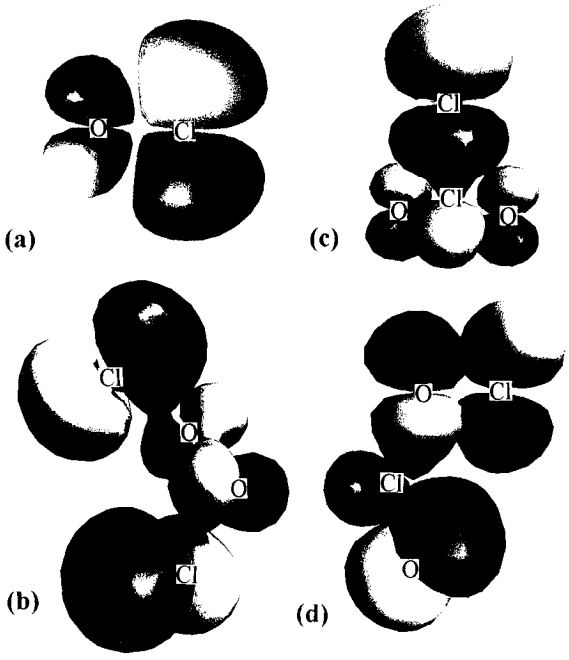

Figure 5. HOMOs of (a) ClO and (b−d) three isomers of Cl_2O_2 obtained from *ab initio* calculations using the UNICHEM program package. Further details are discussed in the text.

$ClClO_2$ that is formed via heterogeneous reactions in the flow tube cannot be excluded completely by the present results. Further experiments using dry and ice-coated flow tube systems are proposed in order to address this question.

Figure 5 shows the HOMOs of ClO (Figure 5a) and the isomers of Cl_2O_2 (Figure 5b−d) that are calculated by using the UNICHEM program package (HF-SCF, 3-21G* basis set with the geometries quoted in ref 6). The calculations indicate that the highest occupied molecular orbital (HOMO) of ClO is of π^* character. It consists mainly of Cl and O p_π orbtials where the charge density is predominantly localized at the chlorine atom. Figure 5b shows that the ClO HOMO structure is hardly changed in the ClOOCl isomer. Thus, the electron density is mostly localized near the chlorine centers, and Coulomb repulsion between both electrons in the HOMO is quite small. As a result, photoionization from this orbital should only have minor effects on the cation bond strength compared to the neutral dimer (see above). Furthermore, there is only a small MO splitting in ClOOCl compared to ClO, which is another indication that the shift in ionization energy should be small. As a consequence, the highest and the second-highest molecular orbitals in ClOOCl are close in energy, as outlined above.

The ionization energies of several other weakly bound dimers have been reported earlier, which can be compared to the IE's of the corresponding monomers. In the case of NO_2/N_2O_4 the adiabatic and vertical ionization energies of the dimer are blue-shifted relative to the monomer: $IE_{adiab}(NO_2) = 9.75$ eV,[39] $IE_{vert}(NO_2) = 11.23$ eV,[42] $IE_{adiab}(N_2O_4) = 10.8$ eV,[39] $IE_{vert}(N_2O_4) = 11.40$ eV,[43] and $D(O_2N-NO_2) = 61.1$ kJ/mol.[44] The blue-shift in adiabatic ionization energies is larger than for the system ClO/Cl_2O_2, which is a result of different chemical bonding in both dimers. Chemical bonding of the NO_2 dimer (N_2O_4) is formed by an interaction of the σ-type HOMOs of both NO_2 moieties.[45] The blue-shift in ionization energy has been rationalized earlier in terms of a balance of the small destabilization due to the "through bond" interaction and a small stabilization derived from the overlap from the cis oxygen atoms.[43] Thus, both weakly bonded dimers show the same qualitative behavior, but there cannot be quantitatively the same shift in ionization energy due to the different electronic structure in both systems.

In contrast, a large red-shift in vertical ionization energy is often observed for strongly bound dimers. As an example, hydrogen peroxide may be regarded as a dimer of two OH radicals. The vertical ionization energy of H_2O_2 is 11.69 eV,[26] whereas that of OH is 13.01 eV.[27] The O−O bond in hydrogen peroxide is much stronger than that in the ClO dimer (D^0(HO−OH) = 204.5 kJ/mol[46]). The charge density in the HOMOs of OH and H_2O_2 is strongly localized at the oxygen sites. As a result, repulsive Coulomb interaction in H_2O_2 increases the energy of the HOMO and consequently the ionization energy of H_2O_2 is significantly lowered compared to the OH radical.

Conclusion

The ionization energy of ClOOCl has been determined for the first time using monochromatic synchrotron radiation in combination with photoionization mass spectrometry. This method is well-suited to study properties of reactive species, such as radical-dimers, which can only be prepared *in situ* without purification. The ionization threshold of Cl_2O_2 is blue-shifted relative to that of ClO by about 0.2 eV. The experimental threshold value of $Cl_2O_2^+$ formation (11.05 ± 0.05 eV) is compared to results from *ab initio* calculations, which aided in identifying the adiabatic ionization energy as well as the isomer that contributes to the mass line of $Cl_2O_2^+$. The results indicate that the most stable isomer ClOOCl is the source of $Cl_2O_2^+$ formation. Therefore, it is possible to derive the heat of formation of $ClOOCl^+$ ($\Delta_f H^0_{298}(ClOOCl^+) = 1203 \pm 12$ kJ/mol) as well as the bond dissociation energy of the singly charged dimer ($D_{298}(ClO-OCl^+) = 48 \pm 18$ kJ/mol). In addition, the occurrence of other less stable Cl_2O_2 isomers, such as $ClClO_2$ and ClOClO, was identified by ionic fragmentation of these species that yielded $OClO^+$.

Acknowledgment. We would like to thank Professor Dr. H. Baumgärtel (Freie Universität Berlin) for his strong encouragement of this work as well as continuous and generous support. We thank Professor Dr. H. Willner (Universität Hannover) and Professor Dr. R.N. Schindler (Universität Kiel) for helpful discussions and for communicating results prior to publication. Financial support by the Freie Universität Berlin, Johannes Gutenberg-Universität Mainz, the Bundesministerium für Bildung, Wissenschaft, Forschung und Technologie (BMBF) (Grant Nos. 05-5 KEFXB5-TP3 and 01 LO 9108/3) and the Fonds der Chemischen Industrie are gratefully acknowledged.

References and Notes

(1) Molina, M. J.; Rowland, F. S. *Nature* **1974**, *249*, 810.

(2) (a) Anderson, J. G.; Brune, W. H.; Proffitt, M. H. *J. Geophys. Res.* **1989**, 11465. (b) Anderson, J. G.; Toohey, D. W.; Brune, W. H. *Science* **1991**, *251*, 39. (c) Waters, J. W.; Froidevaux, L.; Read, W. G.; Manney, G. L.; Elson, L. S.; Flower, D. A.; Jarnot, R.; Harwood, R. S. *Nature* **1993**, *362*, 597.

(3) (a) Crutzen, P. J.; Arnold, F. *Nature* **1986**, *324*, 651. (b) Toon, O. B.; Hamill, P.; Turco, R. P.; Pinto, J. *Geophys. Res. Lett.* **1986**, *13*, 1284. (c) Turco, R. P.; Toon, O. B.; Hamill, P. *J. Geophys. Res.* **1989**, *94*, 16493. (d) Zhang, R.; Jayne, J. T.; Molina, M. J. *J. Phys. Chem.* **1994**, *98*, 867.

(4) Tolbert, M. A. *Science* **1994**, *264*, 527.

(5) (a) Cox, R. A.; Hayman, G. D. *Nature* **1988**, *332*, 796. (b) Trolier, M.; Mauldin, R. L., III; Ravishankara, A. R. *J. Phys. Chem.* **1990**, *94*, 4896.

(6) McGrath, M. P.; Clemitshaw, K. C.; Rowland, F. S.; Hehre, W. J. *J. Phys. Chem.* **1990**, *94*, 6126.

(7) Jensen, F.; Oddershede, J. *J. Phys. Chem.* **1990**, *94*, 2235.

(8) Jacobs, J.; Kronberg, M.; Müller, H. S. P.; Willner, H. *J. Am. Chem. Soc.* **1994**, *116*, 1106.

(9) Burkholder, J. B.; Orlando, J. J.; Howard, C. J. *J. Phys. Chem.* **1990**, *94*, 687.

(10) Huder, K. J.; DeMore, W. B. *J. Phys. Chem.* **1995**, *99*, 3905.

(11) Molina, M. J.; Colussi, A. J.; Molina, L. T.; Schindler, R. N.; Tso, T.-L. *Chem. Phys. Lett.* **1990**, *173*, 310.
(12) DeMore, W. B.; Tschuikow-Roux, E. *J. Phys. Chem.* **1990**, *94*, 5856.
(13) Eberstein, I. J. *Geophys. Res. Lett.* **1990**, *17*, 721.
(14) Bulgin, D. K.; Dyke, J. M.; Jonathan, N. Morris, A. *Mol. Phys.* **1976**, *32*, 1487.
(15) Bulgin, D. K.; Dyke, J. M.; Jonathan, N.; Morris, A. *J. Chem. Soc., Faraday Trans. 2* **1979**, *75*, 456.
(16) Turnipseed, A. A.; Birks, J. W.; Calvert, J. G. *J. Phys. Chem.* **1991**, *95*, 4356.
(17) Wiley, W. C.; McLaren, I. H. *Rev. Sci. Instrum.* **1955**, *26*, 1150.
(18) Rühl, E.; Jochims, H. W.; Schmale, C.; Biller, E.; Simon, M; Baumgärtel, H. *J. Chem. Phys.* **1991**, *95*, 6544.
(19) Rockland, U.; Baumgärtel, H; Rühl, E.; Lösking, O.; Müller, H. S. P.; Willner, H. *Ber. Bunsenges. Phys. Chem.* **1995**, *99*, 969.
(20) Berkowitz, J. *Photoabsorption, Photoionization, and Photoelectron Spectroscopy*; Academic Press: New York, 1979.
(21) Guest, M. F.; Sherwood, P. *GAMESS-UK, Ab Initio Program Package*, SERC Daresbury Laboratory, 1992.
(22) Frisch, M.; Foresman, J.; Frisch, A. *GAUSSIAN 94*, Pittsburgh, 1994.
(23) Werner, H. J.; Knowles, P. J. *MOLPRO Ab Initio Program Package*, University of Sussex, 1994.
(24) Flesch, R.; Wassermann, B.; Rothmund, B.; Rühl, E. *J. Phys. Chem.* **1994**, *98*, 6263.
(25) Rosenstock, H. M.; Draxl, K.; Steiner, B. W.; Herron, J. T. *J. Phys. Chem. Ref. Data* **1977**, *6*, Suppl. 1.
(26) Osafune, K.; Kimura, K. *Chem. Phys. Lett.* **1974**, *25*, 47.
(27) Katsumata, S.; Lloyd, D. R. *Chem. Phys. Lett.* **1977**, *45*, 519.
(28) Robin, M. B. *Higher Excited States of Polyatomic Molecules*; Academic Press: New York, 1974, 1975; Vols. 1 and 2.
(29) (a) Rühl, E.; Jochims, H.-W.; Baumgärtel, H. *Can. J. Chem.* **1985**, *63*, 1949. (b) Rühl, E.; Brutschy, B.; Baumgärtel, H. *Chem. Phys. Lett.* **1989**, *157*, 379.
(30) Lee, T. J.; McMichael Rohlfing, C.; Rice, J. E. *J. Chem. Phys.* **1992**, *97*, 6593.
(31) Stanton, F. J.; Rittby, M. L.; Bartlett, R. J.; Toohey, D. W. *J. Phys. Chem.* **1991**, *95*, 2107.
(32) Stanton, J. F.; Bartlett, R. J. *J. Chem. Phys.* **1993**, *98*, 9335.
(33) Cornford, A. B.; Frost, D. C.; Herring, F. G.; McDowell, C. A. *J. Chem. Phys.* **1971**, *55*, 2820.
(34) Flesch, R; Rühl, E.; Hottmann, K.; Baumgärtel, H. *J. Phys. Chem.* **1993**, *97*, 837.
(35) Schindler, R. N. Proceedings of the 4. Statusseminar des Ozonforschungsprogramms, Bonn, 1994.
(36) Schindler, R. N.; Willner, H. Unpublished results.
(37) Traeger, J. C.; McLoughlin, R. G. *J. Am. Chem. Soc.* **1981**, *103*, 3647.
(38) Abramowitz, S.; Chase, M. W., Jr. *Pure Appl. Chem.* **1991**, *63*, 1449.
(39) Lias, S. G.; Bartmess, J. E.; Liebman, J. F.; Holmes, J. L.; Levin, R. D.; Mallard, W. G. *J. Phys. Chem. Ref. Data* **1988**, *17*, Suppl. 1.
(40) Rockland, U. Ph.D. Thesis, Freie Universität Berlin, 1994.
(41) Wagman, D. D.; Evans, D. H.; Parker, V. B.; Schumm, R. H.; Halow, I; Bailey, S. M.; Churney, K. L.; Nuttall, R. L. *J. Phys. Chem. Ref. Data* **1982**, *11*, Suppl. 2.
(42) Kimura, K.; Katsumata, S.; Achiba, Y.; Yamasaki, T.; Iwata, S. *Handbook of He(I) Photoelectron Spectra of Fundamental Organic Molecules*; Japan Scientific Societies Press: Tokyo, 1981.
(43) Frost, D. C.; McDowell, C. A.; Westwood, N. P. C. *J. Electron Spectrosc. Relat. Phenom.* **1977**, *10*, 293.
(44) Verhoek, F. H.; Daniels, F. *J. Am. Chem. Soc.* **1931**, *53*, 1250.
(45) Ahlrichs, K.; Keil, F. *J. Am. Chem. Soc.* **1974**, *96*, 7515.
(46) Herzberg, G. *Molecular Spectra and Molecular Structure*; Van Nostrand Reinhold: New York, 1966; Vol. 3.

JP9602585